



RELIABILITY OF PLASTIC ROTATION CALCULATIONS FOR DAMAGE ASSESSMENT OF MOMENT-RESISTING FRAMED STRUCTURES

K.K.F. Wong⁽¹⁾

⁽¹⁾ Research Structural Engineer, National Institute of Standards and Technology, kevin.wong@nist.gov

Abstract

Performance-based standards use plastic rotation as an important measure to determine whether the response meets the acceptance criteria for moment-resisting frames. Since plastic rotation is the key parameter in performance-based seismic engineering, the method used to calculate this quantity must be robust and accurate. Although engineers often rely on the plastic rotation output from structural analysis software packages to determine acceptable performance, the actual calculation methods usually depend on the analytical formulations utilized in the particular software. Difficulties in verifying the accuracy of the output results exist because material nonlinearity is often coupled with geometric nonlinearity in the analysis of moment-resisting frames, yet a robust analytical framework for the verification process is currently unavailable because of the lack of analytical theory. To address this problem, an analytical method to calculate the plastic rotations of plastic hinges in moment-resisting frames is presented in this research. The element stiffness matrices are rigorously derived using a member formulation, which includes the coupling of geometric and material nonlinearity effects from the beginning of the derivation. Numerical simulation is performed to calculate the nonlinear responses of structural models subjected to static and dynamic loads. Plastic rotations and other response measures are compared with those obtained using other methods of handling geometric nonlinearity to demonstrate the feasibility of the proposed analytical method.

Keywords: Geometric nonlinearity; material nonlinearity; stability functions; geometric stiffness; structural analysis



1. Introduction

Plastic rotation is one of the most important structural performance metrics for moment-resisting framed structures. Current performance-based standards, such as ASCE/SEI 41 [1], use plastic rotation as the primary performance measure in the assessment process. Relatively large lateral displacement and plastic rotations are expected to occur due to the flexibility of these frames. Therefore, the analysis of moment-resisting framed structures should possess the capability of handling both material nonlinearity and geometric nonlinearity in order to provide the outputs necessary for gauging acceptable performance when large displacements are expected [2-5].

Geometric nonlinearity causes a reduction in stiffness due to the axial compressive force acting on the entire length in the member, while material nonlinearity causes a reduction in stiffness concentrated at the plastic hinges of the member. These two nonlinear phenomena interact with one another in moment-resisting frames, but different structural analysis software packages and algorithms use different assumptions to capture the interaction. The most efficient approach is to handle material and geometric nonlinearity independently. It can be shown that running an algorithm considering material nonlinearity by itself will produce reasonably accurate results. Moreover, separately running an algorithm considering geometric nonlinearity also can produce reasonably accurate results. However, when material nonlinearity is combined with geometric nonlinearity in an analysis, algorithms often neglect the interactions between these nonlinearities, resulting in limited consistency, reduced accuracy, and solution instability. As a result, plastic rotation, as the end product of the analysis, can differ significantly based on the approach taken in the nonlinear algorithm.

One reason for the shortcoming in addressing the nonlinear interaction is that there is no analytical theory that can be used to measure this interaction. Therefore, a numerical solution is often employed that assumes the nonlinear interaction is automatically taken into account when both material and geometric nonlinearities are independently captured and combined. In view of this shortcoming, the present research proposes a method to accurately calculate the plastic rotation while capturing the interaction of material nonlinearity and geometric nonlinearity using an analytical theory based on fundamental principles of structural mechanics. Element stiffness matrices are first derived using a member with plastic hinges subjected to axial compression; therefore, both geometric nonlinearity and material nonlinearity along with their interactions are captured from the beginning of the formulation. The element stiffness matrices are then assembled in the global stiffness matrices to perform both nonlinear static analysis and nonlinear dynamic analysis. Numerical simulations are then performed on simple frames to calculate plastic rotations, and the results are compared with those obtained from other methods of analysis that consider different forms of geometric nonlinearity.

2. Stiffness Matrices for Geometric and Material Nonlinearities

The use of stability functions for analyzing moment-resisting framed structures is here derived to determine the element stiffness matrices of frame members with plastic hinges at both ends. The original theory was first developed for elastic members in the 1960's [6-7] without any consideration of yielding and formation of plastic hinge, but it found limited application because of its complexity in the closed-form solution as compared to those methods of using either the P - Δ stiffness approach [8] or the geometric stiffness approach [9]. However, when large lateral deflections in framed structures are expected, excessive geometric nonlinearity is coupled with excessive material nonlinearity, and the first-order or second-order approximation of the geometric nonlinearity may not be able to capture the nonlinear behavior accurately. Therefore, stability functions are used to investigate the differences in plastic rotation calculations as compared to other geometric nonlinearity formulations.

2.1 Element Stiffness Matrix [\mathbf{k}_i]

Four degrees of freedom (DOFs) are typically used to describe the lateral displacement and rotation at the two ends of a member of moment-resisting frames. To compute the element stiffness matrix \mathbf{k}_i , each of these 4 DOFs is displaced independently by one unit as shown in Fig. 1 while subjected to an axial compressive load P .



Here, V_{1s} , M_{1s} , V_{2s} , and M_{2s} represent the required shear forces and moments at the two ends of the member to cause the lateral displacements and rotations in the prescribed pattern, and $s = 1, \dots, 4$ represents the four cases of unit displacement patterns of the member's deflection.

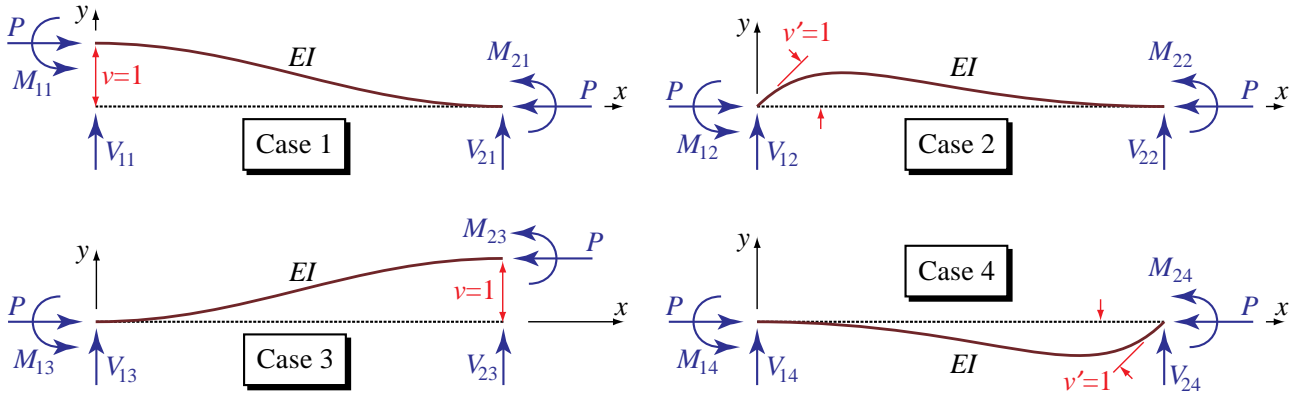


Fig. 1 – Four cases of displacement patterns and the corresponding fixed-end forces

Using the classical Bernoulli-Euler beam theory with homogeneous and isotropic material properties where the moment is proportional to the curvature and plane sections are assumed to remain plane, the governing equilibrium equation describing the deflected shape of the member can be written as

$$(EIv''') + Pv'' = 0 \quad (1)$$

where E is the elastic modulus, I is the moment of inertia, v is the lateral deflection, P is the axial compressive force of the member, and each prime represents taking derivatives of the corresponding variable with respect to the x -direction of the member. By assuming EI is constant along the member, the solution to the fourth-order ordinary differential equation becomes:

$$v = A \sin kx + B \cos kx + Cx + D \quad (2)$$

where $k^2 = P/EI$. Let $\lambda = kL$ to simplify the derivations, where L is the length of the member. The following four cases of boundary conditions (in reverse order) are now considered.

Case 4:

For Case 4 as shown in Fig. 1, imposing the boundary conditions $v(0) = 0$, $v'(0) = 0$, $v(L) = 0$, and $v'(L) = 1$ on Eq. (2) gives

$$v(0) = 0: \quad B + D = 0 \quad (3a)$$

$$v'(0) = 0: \quad kA + C = 0 \quad (3b)$$

$$v(L) = 0: \quad A \sin \lambda + B \cos \lambda + CL + D = 0 \quad (3c)$$

$$v'(L) = 1: \quad kA \cos \lambda - kB \sin \lambda + C = 1 \quad (3d)$$

Solving simultaneously for the constants in Eq. (3) gives

$$A = \frac{L(1 - \cos \lambda)}{\lambda(\lambda \sin \lambda + 2 \cos \lambda - 2)}, \quad B = \frac{L(\sin \lambda - \lambda)}{\lambda(\lambda \sin \lambda + 2 \cos \lambda - 2)}, \quad C = -kA, \quad D = -B \quad (4)$$

Therefore, Eq. (2) along with the constants in Eq. (4) gives the deflected shape for Case 4. The shears (i.e., V_{14} and V_{24}) and moments (i.e., M_{14} and M_{24}) at the two ends of the member (see Fig. 1) are then evaluated using the classical Bernoulli-Euler beam theory formula:

$$M(x) = EIv'' \quad , \quad V(x) = EIv''' + Pv' \quad (5)$$



Now taking derivatives of Eq. (2) and substituting the results into Eq. (5) while using the constants calculated in Eq. (4), the shears and moments at the two ends of the member for Case 4 in Fig. 1 are calculated as:

$$M_{14} = -EIv''(0) = EIk^2 B = \hat{s}\hat{c}EI/L \quad (6a)$$

$$V_{14} = EIv'''(0) + Pv'(0) = -EIk^3 A + P \times 0 = \bar{s}EI/L^2 \quad (6b)$$

$$M_{24} = EIv''(L) = -EIk^2(A \sin \lambda + B \cos \lambda) = \hat{s}EI/L \quad (6c)$$

$$V_{24} = -EIv'''(L) - Pv'(L) = EIk^3(A \cos \lambda - B \sin \lambda) - P \times 1 = -\bar{s}EI/L^2 \quad (6d)$$

where

$$\hat{s} = \frac{\lambda(\sin \lambda - \lambda \cos \lambda)}{2 - 2 \cos \lambda - \lambda \sin \lambda}, \quad \hat{c} = \frac{\lambda - \sin \lambda}{\sin \lambda - \lambda \cos \lambda}, \quad \bar{s} = \hat{s} + \hat{c} = \frac{\lambda^2(1 - \cos \lambda)}{2 - 2 \cos \lambda - \lambda \sin \lambda} \quad (7)$$

The minus signs appear in front of the equations for M_{14} in Eq. (6a) and V_{24} in Eq. (6d) because there is a difference in sign convention between the classical Bernoulli-Euler beam theory and the theory for the stiffness method of structural analysis.

Case 3:

For Case 3 as shown in Fig. 1, imposing the boundary conditions $v(0) = 0$, $v'(0) = 0$, $v(L) = 1$, and $v'(L) = 0$, the constants in Eq. (2) can be solved by using a similar procedure as presented in Case 4 above. Then the shears and moments at the two ends of the member for Case 3 in Fig. 1 are calculated as:

$$M_{13} = -EIv''(0) = -\bar{s}EI/L^2, \quad V_{13} = EIv'''(0) + Pv'(0) = -s'EI/L^3 \quad (8a)$$

$$M_{23} = EIv''(L) = -\bar{s}EI/L^2, \quad V_{23} = -EIv'''(L) - Pv'(L) = s'EI/L^3 \quad (8b)$$

where

$$s' = 2\bar{s} - \lambda^2 = \frac{\lambda^3 \sin \lambda}{2 - 2 \cos \lambda - \lambda \sin \lambda} \quad (9)$$

Case 2:

For Case 2 as shown in Fig. 1, imposing the boundary conditions $v(0) = 0$, $v'(0) = 1$, $v(L) = 0$, and $v'(L) = 0$ on Eq. (2) and following a similar procedure as presented in Cases 3 and 4 above, the shears and moments at the two ends are calculated as:

$$M_{12} = -EIv''(0) = \hat{s}EI/L, \quad V_{12} = EIv'''(0) + Pv'(0) = \bar{s}EI/L^2 \quad (10a)$$

$$M_{22} = EIv''(L) = \hat{s}\hat{c}EI/L, \quad V_{22} = -EIv'''(L) - Pv'(L) = -\bar{s}EI/L^2 \quad (10b)$$

Case 1:

Finally for Case 1 as shown in Fig. 1, imposing the boundary conditions $v(0) = 1$, $v'(0) = 0$, $v(L) = 0$, and $v'(L) = 0$ on Eq. (2) and following a similar procedure as presented in Cases 3 and 4 above, the shears and moments at the two ends are calculated as:

$$M_{11} = -EIv''(0) = \bar{s}EI/L^2, \quad V_{11} = EIv'''(0) + Pv'(0) = s'EI/L^3 \quad (11a)$$

$$M_{21} = EIv''(L) = \bar{s}EI/L^2, \quad V_{21} = -EIv'''(L) - Pv'(L) = -s'EI/L^3 \quad (11b)$$

In summary, based on Eqs. (6), (8), (10), and (11) for the above four cases, the element stiffness matrix of the i^{th} member \mathbf{k}_i for bending after incorporating axial compressive force using stability functions becomes:



$$\mathbf{k}_i^{SF} = \frac{EI}{L^3} \begin{bmatrix} s' & \bar{s}L & -s' & \bar{s}L \\ \bar{s}L & \hat{s}L^2 & -\bar{s}L & \hat{s}L^2 \\ -s' & -\bar{s}L & s' & -\bar{s}L \\ \bar{s}L & \hat{s}L^2 & -\bar{s}L & \hat{s}L^2 \end{bmatrix} \begin{matrix} \leftarrow v(0) \\ \leftarrow v'(0) \\ \leftarrow v(L) \\ \leftarrow v'(L) \end{matrix} \quad (12)$$

where the superscript ‘SF’ is used to denote that the element stiffness matrix \mathbf{k}_i is computed by using the stability functions method.

Linearization of Eq. (12) can be performed by using Taylor series expansion on each term of the element stiffness matrix and truncating higher-order terms. Doing so gives

$$\mathbf{k}_i^{GS} = \frac{EI}{L^3} \begin{bmatrix} 12 & 6L & -12 & 6L \\ 6L & 4L^2 & -6L & 2L^2 \\ -12 & -6L & 12 & -6L \\ 6L & 2L^2 & -6L & 4L^2 \end{bmatrix} - \begin{bmatrix} 6P/5L & P/10 & -6P/5L & P/10 \\ P/10 & 2PL/15 & -P/10 & -PL/30 \\ -6P/5L & -P/10 & 6P/5L & -P/10 \\ P/10 & -PL/30 & -P/10 & 2PL/15 \end{bmatrix} \begin{matrix} \leftarrow v(0) \\ \leftarrow v'(0) \\ \leftarrow v(L) \\ \leftarrow v'(L) \end{matrix} \quad (13)$$

where the first matrix in Eq. (13) represents that classic stiffness matrix without considering any geometric nonlinearity, and the second matrix represents the geometric stiffness. The superscript ‘GS’ is used to denote that the element stiffness matrix \mathbf{k}_i is computed by using the geometric stiffness method. Finally, the element stiffness matrix in Eq. (13) can be further simplified by retaining only the large P - Δ stiffness while ignoring the small P - δ effect. Doing so gives

$$\mathbf{k}_i^{PD} = \frac{EI}{L^3} \begin{bmatrix} 12 & 6L & -12 & 6L \\ 6L & 4L^2 & -6L & 2L^2 \\ -12 & -6L & 12 & -6L \\ 6L & 2L^2 & -6L & 4L^2 \end{bmatrix} - \begin{bmatrix} P/L & 0 & -P/L & 0 \\ 0 & 0 & 0 & 0 \\ -P/L & 0 & P/L & 0 \\ 0 & 0 & 0 & 0 \end{bmatrix} \begin{matrix} \leftarrow v(0) \\ \leftarrow v'(0) \\ \leftarrow v(L) \\ \leftarrow v'(L) \end{matrix} \quad (14)$$

where the superscript ‘PD’ is used to denote that the element stiffness matrix \mathbf{k}_i is computed by using the P - Δ stiffness method.

2.2 Element Stiffness Matrix [\mathbf{k}'_i]

The second element stiffness matrix, \mathbf{k}'_i , relates the plastic rotations at the plastic hinge locations (PHLs) of the i^{th} member with the restoring forces applied at the DOFs. Two plastic hinges typically occur at the two ends of the member, and they are labeled as ‘a’ for plastic hinge at the ‘1’ end and ‘b’ for plastic hinge at the ‘2’ end as shown in Fig. 2. The transpose of the \mathbf{k}'_i matrix is here constructed. This $\mathbf{k}'_i{}^T$ matrix relates the lateral displacements and rotations at the two ends of the member (i.e., the four cases of unit displacements presented in Section 2.1) with the moments at the PHLs (i.e., M_{as} and M_{bs} , $s = 1, \dots, 4$).

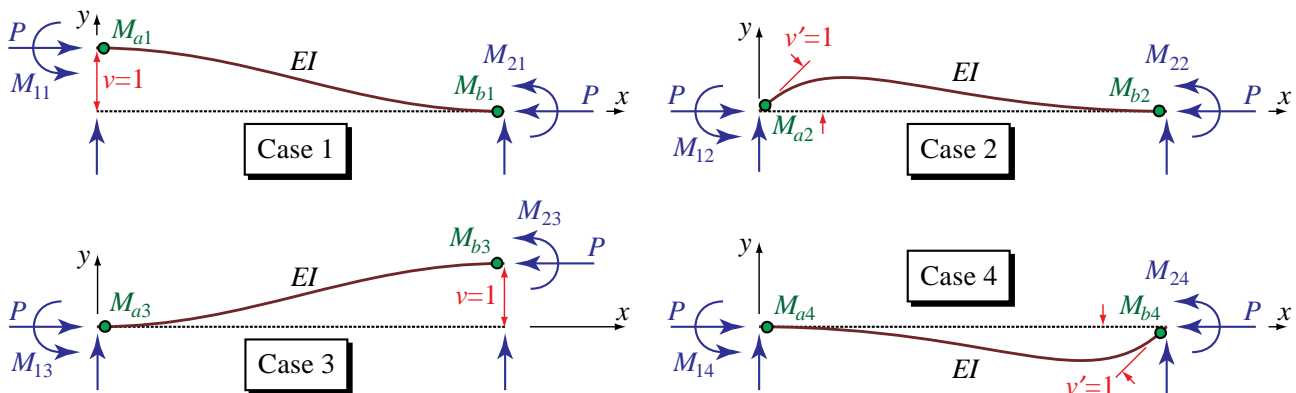


Fig. 2 – Displacement patterns for computation of moments at the PHLs



Consider each of the four cases of unit displacements for the member as shown in Fig. 2, where the moments at the plastic hinges ‘a’ and ‘b’ (i.e., M_{as} and M_{bs} , $s=1,\dots,4$) represent the desired quantities. By joint equilibrium based on Fig. 2, these moments for each of the four cases can be evaluated directly as presented in the following sub-sections.

Case 1:

For Case 1 as shown in Fig. 2, imposing the boundary conditions $v(0)=1$, $v'(0)=0$, $v(L)=0$, and $v'(L)=0$ gives the moments M_{a1} and M_{b1} (also see Eq. (11)) as:

$$M_{a1} = M_{11} = \bar{s}EI/L^2 \quad , \quad M_{b1} = M_{21} = \bar{s}EI/L^2 \quad (15)$$

Case 2:

For Case 2 as shown in Fig. 2, imposing the boundary conditions $v(0)=0$, $v'(0)=1$, $v(L)=0$, and $v'(L)=0$ gives the moments M_{a2} and M_{b2} (also see Eq. (10)) as:

$$M_{a2} = M_{12} = \hat{s}EI/L \quad , \quad M_{b2} = M_{22} = \hat{s}EI/L \quad (16)$$

Case 3:

For Case 3 as shown in Fig. 2, imposing the boundary conditions $v(0)=0$, $v'(0)=0$, $v(L)=1$, and $v'(L)=0$ gives the moments M_{a3} and M_{b3} (also see Eq. (8)) as

$$M_{a3} = M_{13} = -\bar{s}EI/L^2 \quad , \quad M_{b3} = M_{23} = -\bar{s}EI/L^2 \quad (17)$$

Case 4:

Finally, for Case 4 as shown in Fig. 2, imposing the boundary conditions $v(0)=0$, $v'(0)=0$, $v(L)=0$, and $v'(L)=1$ gives the moments M_{a4} and M_{b4} (also see Eq. (6)) as

$$M_{a4} = M_{14} = \hat{s}EI/L \quad , \quad M_{b4} = M_{24} = \hat{s}EI/L \quad (18)$$

In summary from Eqs. (15) to (18), the transpose of stiffness matrix \mathbf{k}'_i for the i^{th} member becomes

$$\mathbf{k}'_i{}^T = \begin{bmatrix} M_{a1} & M_{a2} & M_{a3} & M_{a4} \\ M_{b1} & M_{b2} & M_{b3} & M_{b4} \end{bmatrix} = \begin{bmatrix} \bar{s}EI/L^2 & \hat{s}EI/L & -\bar{s}EI/L^2 & \hat{s}EI/L \\ \bar{s}EI/L^2 & \hat{s}EI/L & -\bar{s}EI/L^2 & \hat{s}EI/L \end{bmatrix} \begin{matrix} \leftarrow \theta''_a \\ \leftarrow \theta''_b \end{matrix} \quad (19)$$

Once the $\mathbf{k}'_i{}^T$ matrix in Eq. (19) is derived, the \mathbf{k}'_i matrix can be written as:

$$\mathbf{k}'_i{}^{SF} = \begin{bmatrix} V_{1a} & V_{1b} \\ M_{1a} & M_{1b} \\ V_{2a} & V_{2b} \\ M_{2a} & M_{2b} \end{bmatrix} = \begin{bmatrix} M_{a1} & M_{b1} \\ M_{a2} & M_{b2} \\ M_{a3} & M_{b3} \\ M_{a4} & M_{b4} \end{bmatrix} = \begin{bmatrix} \bar{s}EI/L^2 & \bar{s}EI/L^2 \\ \hat{s}EI/L & \hat{s}EI/L \\ -\bar{s}EI/L^2 & -\bar{s}EI/L^2 \\ \hat{s}EI/L & \hat{s}EI/L \end{bmatrix} \begin{matrix} \leftarrow v(0) \\ \leftarrow v'(0) \\ \leftarrow v(L) \\ \leftarrow v'(L) \end{matrix} \quad (20)$$

where the superscript ‘SF’ is used to denote that the element stiffness matrix \mathbf{k}_i is computed by using the stability functions method.

2.3 Element Stiffness Matrix [\mathbf{k}''_i]

The third element stiffness matrix, \mathbf{k}''_i , relates the moments at PHLs ‘a’ and ‘b’ of the i^{th} member with a unit plastic rotation at each of these PHLs. To determine the \mathbf{k}''_i matrix, the goal is to compute the plastic hinge moments M_{aa} , M_{ab} , M_{ba} , and M_{bb} due to a unit plastic rotation at either ‘a’ or ‘b’ as shown in Fig. 3. These moments for each of the two cases can be evaluated directly by using joint equilibrium as presented in the following sub-sections.

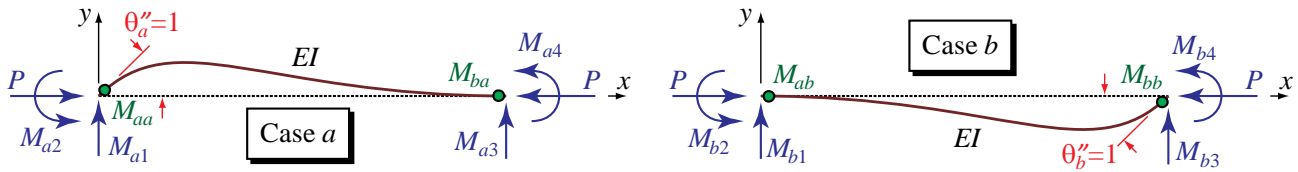


Fig. 3 – Displacement patterns for computation of moments due to unit plastic rotations

Case ‘a’:

For Case ‘a’ of Fig. 3, imposing a unit plastic rotation $\theta_a'' = 1$ and $\theta_b'' = 0$ gives (see Eq. (20))

$$M_{aa} = M_{a2} = \hat{\sigma}EI/L \quad , \quad M_{ba} = M_{a4} = \hat{\sigma}\hat{c}EI/L \quad (21)$$

Case ‘b’:

For Case ‘b’ of Fig. 3, imposing a unit plastic rotation $\theta_a'' = 0$ and $\theta_b'' = 1$ gives (see Eq. (20))

$$M_{ab} = M_{b2} = \hat{\sigma}\hat{c}EI/L \quad , \quad M_{bb} = M_{b4} = \hat{\sigma}EI/L \quad (22)$$

Therefore, in summary from Eqs. (21) and (22), the element stiffness matrix \mathbf{k}_i'' for the i^{th} member becomes

$$\mathbf{k}_i''^{SF} = \begin{bmatrix} \hat{\sigma}EI/L & \hat{\sigma}\hat{c}EI/L \\ \hat{\sigma}\hat{c}EI/L & \hat{\sigma}EI/L \end{bmatrix} \begin{matrix} \leftarrow \theta_a'' \\ \leftarrow \theta_b'' \end{matrix} \quad (23)$$

where the superscript ‘SF’ is used to denote that the element stiffness matrix \mathbf{k}_i is computed by using the stability functions method.

2.4 Global Stiffness Matrices

By using the element stiffness matrices computed in Eqs. (12), (20), and (23), the assembly of these matrices into the global stiffness matrices \mathbf{K} , \mathbf{K}' , and \mathbf{K}'' follows a straightforward procedure. A number of textbooks have discussed this procedure in great detail [10]. Consider a framed structure having a total of n DOFs and m PHLs, the resulting global stiffness matrices can be obtained by this assembly procedure and are often written in the form:

$$\mathbf{K} = \begin{bmatrix} \text{Collection of } \mathbf{k}_i \end{bmatrix}_{n \times n} \quad , \quad \mathbf{K}' = \begin{bmatrix} \text{Collection of } \mathbf{k}_i' \end{bmatrix}_{n \times m} \quad , \quad \mathbf{K}'' = \begin{bmatrix} \text{Collection of } \mathbf{k}_i'' \end{bmatrix}_{m \times m} \quad (24)$$

The resulting stiffness equation for computing the response of the structure with both geometric and material nonlinearities can therefore be written as [11]:

$$\begin{bmatrix} F_1 \\ \vdots \\ F_n \\ M_1 \\ \vdots \\ M_m \end{bmatrix} = \begin{bmatrix} \mathbf{K} & \mathbf{K}' \\ \mathbf{K}'^T & \mathbf{K}'' \end{bmatrix} \begin{bmatrix} x_1 \\ \vdots \\ x_n \\ -\theta_1'' \\ \vdots \\ -\theta_m'' \end{bmatrix} \quad (25)$$

where F_i and x_i ($i=1,\dots,n$) denote respectively the global applied forces and displacements at the DOFs, and M_i and θ_i'' ($i=1,\dots,m$) denote respectively the local moments and plastic rotations at the PHLs.

3. Numerical Illustration Using Static Loading

Consider a two-dimensional frame as shown in Fig. 4(a) with one column member and one beam member, where both members have the same elastic modulus E , moment of inertia I , and length L . The column is subjected to a constant axial force P , and the frame is subjected to a lateral force F_o . Assume both members are axially rigid. The resulting structural model is a three-DOF system (labeled here as x_1 , x_2 , and x_3) as shown in Fig. 4(a). In addition, three PHLs are identified as shown in Fig. 4(a) with the corresponding component models for the moment vs. plastic rotation relationship as shown in Fig. 4(b). The moment vs. plastic rotation relationships exhibit strain hardening behaviors with θ_i'' denoting plastic rotation, M_i the moment, M_{Yi} the yield moment, and k_{ti} the hardening stiffness of the i^{th} plastic hinge, where $i = 1, 2, 3$.

Based on these labeled DOFs and PHLs, Eq. (25) becomes

$$\begin{bmatrix} F_o \\ 0 \\ 0 \\ M_1 \\ M_2 \\ M_3 \end{bmatrix} = \begin{bmatrix} s'EI/L^3 & \bar{s}EI/L^2 & 0 & \bar{s}EI/L^2 & \bar{s}EI/L^2 & 0 \\ 0 & \bar{s}EI/L^2 & (\hat{s}+4)EI/L & \hat{s}\hat{c}EI/L & \hat{s}EI/L & 4EI/L \\ 0 & 0 & 2EI/L & 4EI/L & 0 & 2EI/L \\ \hline \bar{s}EI/L^2 & \hat{s}\hat{c}EI/L & 0 & \hat{s}EI/L & \hat{s}\hat{c}EI/L & 0 \\ \bar{s}EI/L^2 & \hat{s}EI/L & 0 & \hat{s}\hat{c}EI/L & \hat{s}EI/L & 0 \\ 0 & 4EI/L & 2EI/L & 0 & 0 & 4EI/L \end{bmatrix} \begin{bmatrix} x_1 \\ x_2 \\ x_3 \\ -\theta_1'' \\ -\theta_2'' \\ -\theta_3'' \end{bmatrix} \quad (26)$$

where \hat{s} , \hat{c} and \bar{s} are defined in Eq. (7) and s' is defined in Eq. (9) for Member 1 as shown in Fig. 4(a).

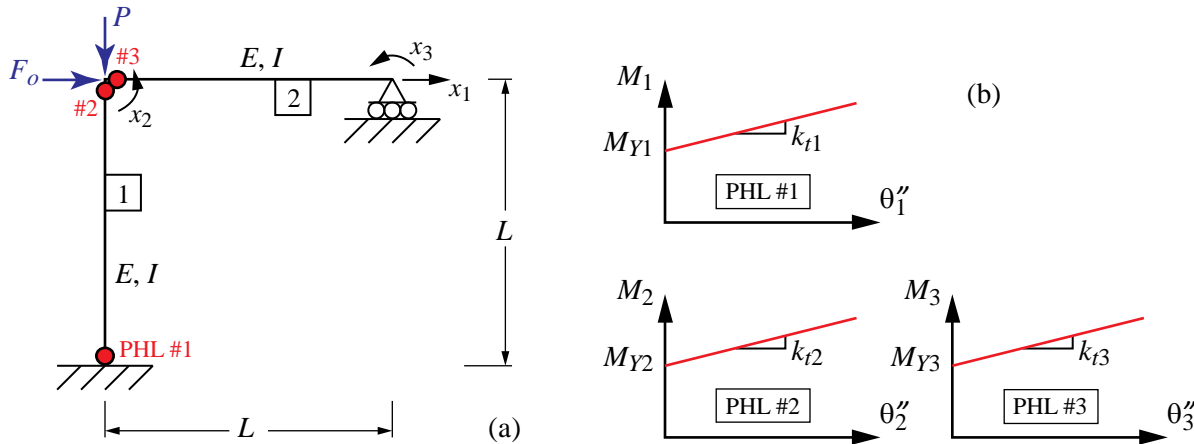


Fig. 4 – Moment frame with 3 degrees of freedom and 3 plastic hinge locations

To perform analysis on the frame with both geometric and material nonlinearities, let the applied force as shown in Fig. 5(a) be $F_o = 48F$ and $P = 0.3EI/L^2$. Assume a post-yield stiffness of $k_{t1} = k_{t2} = k_{t3} = 3EI/L$ for all three plastic hinges. Let the yield moments of the plastic hinges be $M_{Y1} = 18FL$, $M_{Y2} = 15FL$, and $M_{Y3} = 25FL$. This gives the component models of moment vs. plastic rotation relationships for the 3 PHLs as

$$\text{if } \begin{cases} |M_1| \leq 18FL \\ |M_1| > 18FL \end{cases} \text{ then } \begin{cases} \theta_1'' = 0 \\ M_1 = 18FL + 3EI\theta_1''/L \end{cases} \quad (27a)$$

$$\text{if } \begin{cases} |M_2| \leq 15FL \\ |M_2| > 15FL \end{cases} \text{ then } \begin{cases} \theta_2'' = 0 \\ M_2 = 15FL + 3EI\theta_2''/L \end{cases} \quad (27b)$$

$$\text{if } \begin{cases} |M_3| \leq 25FL \\ |M_3| > 25FL \end{cases} \text{ then } \begin{cases} \theta_3'' = 0 \\ M_3 = 25FL + 3EI\theta_3''/L \end{cases} \quad (27c)$$



3.1 Step 1

Equation (26) is now used to perform structural analysis. First assume that the frame remains elastic under the applied load (i.e., $\theta_1'' = \theta_2'' = \theta_3'' = 0$). The first three equations of Eq. (26) can be used to solve for the displacements at the DOFs, and the last three equations of Eq. (26) can be used to compute the resulting moments. Doing so gives

$$\begin{Bmatrix} x_1 \\ x_2 \\ x_3 \end{Bmatrix} = \begin{Bmatrix} 7.3630FL^3/EI \\ -6.3158FL^2/EI \\ 3.1579FL^2/EI \end{Bmatrix}, \quad \begin{Bmatrix} M_1 \\ M_2 \\ M_3 \end{Bmatrix} = \begin{Bmatrix} 31.2616FL \\ 18.9474FL \\ -18.9474FL \end{Bmatrix} \quad (28)$$

Since the computed moments of $M_1 = 31.2616FL$ and $M_2 = 18.9474FL$ are both larger than the corresponding yield moment, this indicates that both PHL #1 and PHL #2 have yielded.

3.2 Step 2

After determining that both PHLs #1 and #2 have yielded due to the applied force of $F_o = 48F$, this step begins by directly assuming that both PHLs #1 and #2 have yielded. The moment vs. plastic rotation relationships in Eq. (27) become

$$M_1 = 18FL + 3EI\theta_1''/L, \quad M_2 = 15FL + 3EI\theta_2''/L \quad (29)$$

and $\theta_3'' = 0$ is still assumed. Then extracting the first five equations in Eq. (26) gives

$$\begin{Bmatrix} 48F \\ 0 \\ 0 \\ M_1 \\ M_2 \end{Bmatrix} = \begin{bmatrix} 11.64EI/L^3 & 5.97EI/L^2 & 0 & 5.97EI/L^2 & 2.01EI/L \\ 5.97EI/L^2 & 7.96EI/L & 2EI/L & 5.97EI/L^2 & 3.96EI/L \\ 0 & 2EI/L & 4EI/L & 0 & 0 \\ 5.97EI/L^2 & 5.97EI/L^2 & 0 & 3.96EI/L & 2.01EI/L \\ 2.01EI/L & 3.96EI/L & 0 & 2.01EI/L & 3.96EI/L \end{bmatrix} \begin{Bmatrix} x_1 \\ x_2 \\ x_3 \\ -\theta_1'' \\ -\theta_2'' \end{Bmatrix} \quad (30)$$

Now substituting Eq. (29) into Eq. (30), the stiffness equation becomes

$$\begin{Bmatrix} 48F \\ 0 \\ 0 \\ 18FL \\ 15FL \end{Bmatrix} = \begin{bmatrix} 11.64EI/L^3 & 5.97EI/L^2 & 0 & 5.97EI/L^2 & 2.01EI/L \\ 5.97EI/L^2 & 7.96EI/L & 2EI/L & 5.97EI/L^2 & 3.96EI/L \\ 0 & 2EI/L & 4EI/L & 0 & 0 \\ 5.97EI/L^2 & 5.97EI/L^2 & 0 & 6.96EI/L & 2.01EI/L \\ 2.01EI/L & 3.96EI/L & 0 & 2.01EI/L & 6.96EI/L \end{bmatrix} \begin{Bmatrix} x_1 \\ x_2 \\ x_3 \\ -\theta_1'' \\ -\theta_2'' \end{Bmatrix} \quad (31)$$

Note that by substituting M_1 and M_2 into Eq. (30), the left hand side of Eq. (31) becomes all known quantities, and the unknown quantities are the DOFs and PHLs on the right hand side of the equation.

Solving for the unknown quantities in Eq. (31) gives

$$\begin{Bmatrix} x_1 \\ x_2 \\ x_3 \\ -\theta_1'' \\ -\theta_2'' \end{Bmatrix} = \begin{Bmatrix} 10.8184FL^3/EI \\ -6.9710FL^2/EI \\ 3.4855FL^2/EI \\ -4.1108FL^2/EI \\ -1.9710FL^2/EI \end{Bmatrix} \quad (32)$$

Then the moments at each plastic hinge are calculated using the last three equations of Eq. (26), i.e.,



$$\begin{Bmatrix} M_1 \\ M_2 \\ M_3 \end{Bmatrix} = \begin{bmatrix} 5.97EI/L^2 & 2.01EI/L & 0 & 3.96EI/L & 2.01EI/L \\ 5.97EI/L^2 & 3.96EI/L & 0 & 2.01EI/L & 3.96EI/L \\ 0 & 4EI/L & 2EI/L & 0 & 0 \end{bmatrix} \begin{Bmatrix} 10.8184FL^3/EI \\ -6.9710FL^2/EI \\ 3.4855FL^2/EI \\ -4.1108FL^2/EI \\ -1.9710FL^2/EI \end{Bmatrix} = \begin{Bmatrix} 30.3325FL \\ 20.9130FL \\ -20.9130FL \end{Bmatrix} \quad (33)$$

Since the computed moments for M_1 and M_2 are both larger than the corresponding yield moment, this means the original assumption is correct. Therefore, in summary, the calculated responses are

$$\begin{Bmatrix} x_1 \\ x_2 \\ x_3 \end{Bmatrix} = \begin{Bmatrix} 10.8184FL^3/EI \\ -6.9710FL^2/EI \\ 3.4855FL^2/EI \end{Bmatrix}, \quad \begin{Bmatrix} M_1 \\ M_2 \\ M_3 \end{Bmatrix} = \begin{Bmatrix} 30.3325FL \\ 20.9130FL \\ -20.9130FL \end{Bmatrix}, \quad \begin{Bmatrix} \theta_1'' \\ \theta_2'' \\ \theta_3'' \end{Bmatrix} = \begin{Bmatrix} 4.1108FL^2/EI \\ 1.9710FL^2/EI \\ 0 \end{Bmatrix} \quad (34)$$

3.3 Results from Using Different Stiffness Matrices

Sections 3.1 and 3.2 demonstrated the procedure for calculating the response of the frame with both geometric and material nonlinearities. Similar procedures can be performed with a variation of stiffness matrices, such as using the geometric stiffness in Eq. (13) or the P - Δ stiffness in Eq. (14). By using the geometric stiffness, the responses are calculated as

$$\begin{Bmatrix} x_1 \\ x_2 \\ x_3 \end{Bmatrix} = \begin{Bmatrix} 10.8183FL^3/EI \\ -6.9709FL^2/EI \\ 3.4854FL^2/EI \end{Bmatrix}, \quad \begin{Bmatrix} M_1 \\ M_2 \\ M_3 \end{Bmatrix} = \begin{Bmatrix} 30.3328FL \\ 20.9127FL \\ -20.9127FL \end{Bmatrix}, \quad \begin{Bmatrix} \theta_1'' \\ \theta_2'' \\ \theta_3'' \end{Bmatrix} = \begin{Bmatrix} 4.1109FL^2/EI \\ 1.9709FL^2/EI \\ 0 \end{Bmatrix} \quad (35)$$

and by using the P - Δ stiffness, the responses are calculated as

$$\begin{Bmatrix} x_1 \\ x_2 \\ x_3 \end{Bmatrix} = \begin{Bmatrix} 10.7834FL^3/EI \\ -6.9493FL^2/EI \\ 3.4747FL^2/EI \end{Bmatrix}, \quad \begin{Bmatrix} M_1 \\ M_2 \\ M_3 \end{Bmatrix} = \begin{Bmatrix} 30.3871FL \\ 20.8479FL \\ -20.8479FL \end{Bmatrix}, \quad \begin{Bmatrix} \theta_1'' \\ \theta_2'' \\ \theta_3'' \end{Bmatrix} = \begin{Bmatrix} 4.1290FL^2/EI \\ 1.9493FL^2/EI \\ 0 \end{Bmatrix} \quad (36)$$

Comparing the results in Eq. (35) with those in Eq. (34) shows that the use of geometric stiffness approximates stability functions very well. But the comparison between Eq. (36) and Eq. (34) shows that there is a larger difference, especially in the calculation of the plastic rotations where the error is about 1% for the simple frame with statically applied load only.

4. Numerical Illustration Using Dynamic Loading

Consider the one-story one-bay moment-resisting frame as shown in Fig. 5(a) with members assumed to be axially rigid. This frame has a total of 3 DOFs (i.e., $n=3$) and 6 PHLs (i.e., $m=6$) as shown in the figure. Assume that the frame has a mass of $m=318.7$ Mg and a damping of 0%. Also, let $E=200$ GPa, $I_b=I_c=4.995 \times 10^8$ mm⁴, $L_b=7.62$ m, $L_c=4.57$ m, and $P=5,338$ kN. Assume that the plastic hinges exhibit elastic-plastic behavior with moment capacities of $M_b=3,130$ kN-m for the beam and $M_c=3,909$ kN-m for the two columns. The frame is then subjected to the 1995 Kobe earthquake ground motion as shown in Fig. 5(b) but magnified with a scale factor of 1.3 to produce a larger response with more yielding at the plastic hinges, and Fig. 6 shows the horizontal displacement response of the floor using the stability functions (SF) method. In addition, results from a commercial software package developed based on the geometric stiffness (GS) method and from another commercial software package developed based on the P - Δ stiffness (PD) are also presented in the figure as a comparison. As shown in Fig. 6, consistency in the model among various algorithms is achieved based on the observation at the first few seconds of the response history, but the responses deviates once yielding occurs in the models.

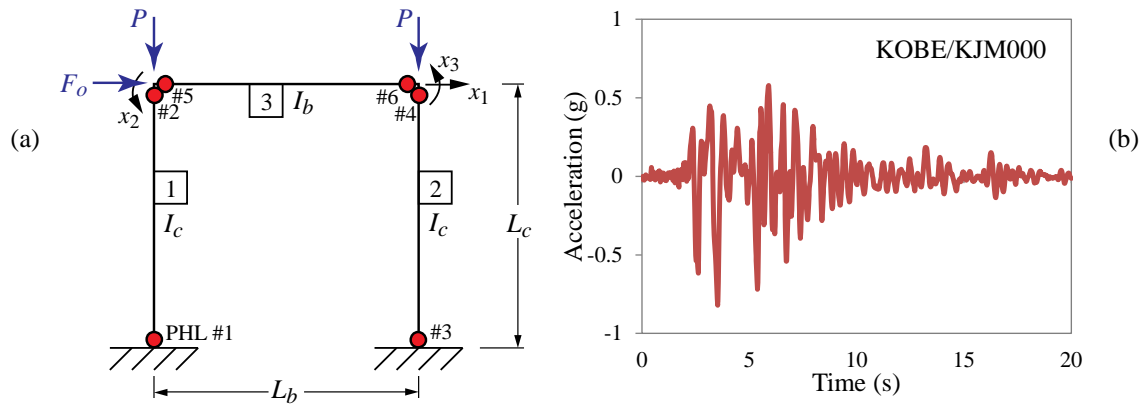


Fig. 5 – One-story one-bay moment-resisting steel frame subjected to the 1995 Kobe earthquake

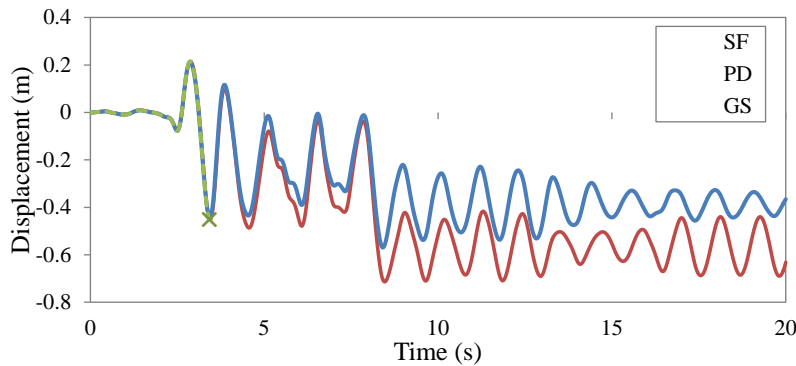


Fig. 6 – Displacement responses of the frame using various geometric nonlinearity formulations with non-convergence in the solution algorithm for GS at 3.46 seconds

The plastic rotation responses at selected plastic hinges are presented in Fig. 7. By comparing SF with PD in Fig. 7, it can be seen that even though the local plastic rotation responses change suddenly (i.e., jumps) due to yielding at the same time steps, the magnitudes of the changes are different. Given the expected accuracy of SF that it is analytically derived, this suggests that the $P-\Delta$ stiffness method may not be a good approximation when plastic rotation is accumulated over time, such as in the case of a dynamic analysis. At the same time, comparing SF and PD with GS in Fig. 7 shows that the non-convergence issue is only found in GS, indicating that a fundamental problem exists in either GS or the software package itself. This may be attributed to the difficulty of incorporating geometric stiffness in a dynamic analysis, where update in stiffness due to material nonlinearity causes non-convergence in the solution algorithm that can only account for geometric nonlinearity. However, further research is needed to examine why such non-convergence exists.

5. Conclusion

Plastic rotation in moment-resisting frame is an important parameter for assessing structural performance under seismic actions, and therefore it needs to be calculated correctly. In this research, fundamental principles were used to derive the stiffness matrices of a member with plastic hinges subjected to an axial load to capture the interaction between geometric nonlinearity and material nonlinearity using stability functions. This results in a rigorous method for calculating the plastic rotation demand of framed structures for both nonlinear static analysis and nonlinear dynamic analysis. Comparing the results using stability functions with other methods for handling geometric nonlinearity shows that the present approach has the advantage for being theoretically derived, and therefore it is believed to be of higher accuracy whenever there is a discrepancy of results. However, further research is necessary to explain why there is such a discrepancy, especially for the case of nonlinear dynamic analysis.

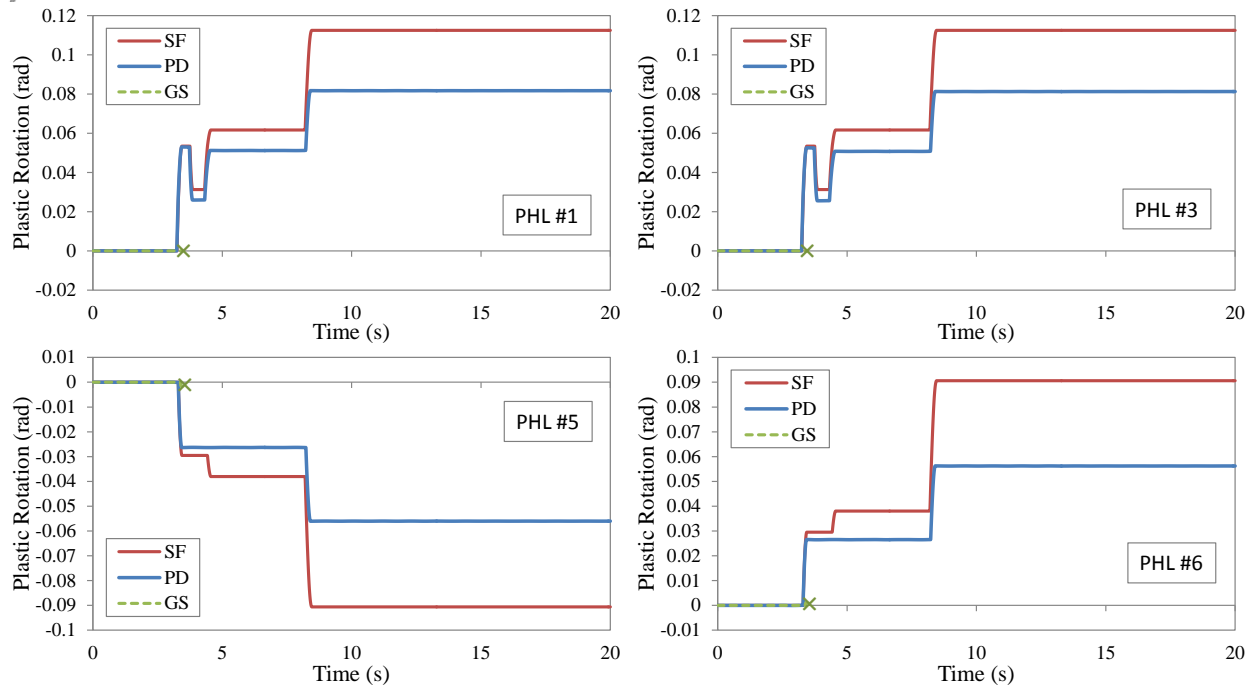


Fig. 7 – Plastic rotation responses at selected PHLs using various geometric nonlinearity formulations with non-convergence in the solution algorithm for GS at 3.46 seconds

6. Disclaimer

No formal investigation to evaluate potential sources of uncertainty or error, or whether multiple sources of error are correlated, was included in this study. The question of uncertainties in the analytical models, solution algorithms, material properties and as-built final dimensions and positions of members versus design configurations employed in analysis are beyond the scope of the work reported here.

7. References

- [1] ASCE/SEI 41-13 (2013): *Seismic Evaluation and Retrofit of Existing Buildings*, American Society of Civil Engineers, Reston, VA, USA.
- [2] Lignos DG, Krawinkler H, Whittaker AS (2011): Prediction and validation of sidesway collapse of two scale models of a 4-story steel moment frame. *Earthquake Engineering and Structural Dynamics*, **40** (7), 807-825.
- [3] Grigorian M, Grigorian CE (2012): Lateral displacements of moment frames at incipient collapse. *Engineering Structures*, **44**, 174-185.
- [4] Eads L, Miranda E, Krawinkler H, Lignos DG (2013): An efficient method for estimating the collapse risk of structures in seismic regions. *Earthquake Engineering and Structural Dynamics*, **42** (1), 25-41.
- [5] Domizio M, Ambrosini D, Curadelli O (2015): Experimental and numerical analysis to collapse of a framed structure subjected to seismic loading. *Engineering Structures*, **82**, 22-32.
- [6] Timoshenko SP, Gere JM (1961): *Theory of Elastic Stability*, 2nd Edition, McGraw Hill, NY, USA.
- [7] Bazant ZP, Cedolin L (2003): *Stability of Structures*, Dover Publication, NY, USA.
- [8] Powell GH (2010): *Modeling for Structural Analysis: Behavior and Basics*, Computers and Structures Inc., CA, USA.
- [9] Wilson E (2010): *Static and Dynamic Analysis of Structures: A Physical Approach with Emphasis on Earthquake Engineering*, 4th Edition, Computer and Structures Inc., CA, USA.
- [10] McGuire W, Gallagher RH, Ziemian RD (2000): *Matrix Structural Analysis*, John Wiley and Sons, NY, USA.
- [11] Wong KKF, Yang R (1999): Inelastic dynamic response of structures using force analogy method. *Journal of Engineering Mechanics ASCE*, **125** (10), 1190-1199.